Atmos. Chem. Phys. Discuss., https://doi.org/10.5194/acp-2018-1133
Manuscript under review for journal Atmos. Chem. Phys.
Discussion started: 3 January 2019

Atmospheric Chemistry and Physics Discussions

Verification of anthropogenic VOC emission inventory through ambient measurements and satellite retrievals

Jing Li[1,2], Yufang Hao[1], Maimaiti Simayi[1], Yuqi Shi[1], Ziyan Xi[1], and Shaodong Xie[1]

[1]College of Environmental Sciences and Engineering, State Key Joint Laboratory of Environmental Simulation and Pollution Control, Peking University, Beijing, 100871, PR China
[2]Department of Environmental Health, Harvard T.H. Chan School of Public Health, Boston, 02215, USA

Correspondence to: Shaodong Xie (xiesd@pku.edu.cn)

Abstract. Improving the accuracy of the anthropogenic volatile organic compound (VOC) emission inventory is essential for reducing air pollution. In this study, we established an emission inventory of anthropogenic VOCs in the Beijing–Tianjin–Hebei (BTH) region of China for 2015 based on the emission factor (EF) method. Online ambient VOC observations were conducted in one urban area of Beijing in January, April, July, and October, which respectively represented winter, spring, summer, and autumn in 2015. Furthermore, the developed emission inventory was evaluated by a comprehensive verification system based on the measurements and satellite retrieval results. Firstly, emissions of the individual species of the emission inventory were evaluated according to the ambient measurements and emission ratios versus carbon monoxide (CO). Secondly, the source structure of the emission inventory was evaluated using source appointment with the Positive Matrix Factorization (PMF) model. Thirdly, the spatial distribution of the developed emission inventory was evaluated by a satellite-derived emission inventory. According to the results of the emission inventory, the total anthropogenic VOC emissions in the BTH region were 3277.66 Gg in 2015. Online measurements showed that the average mixing ratio of VOCs in Beijing was approximately 49.94 ppbv in 2015, ranging from 10.67 ppbv to 245.54 ppbv. The annual emissions of non-methane hydrocarbons (NMHCs) derived from the measurements were significantly consistent with the results of the emission inventory. Based on the PMF results and the emission inventory, it is clearly evident that vehicle-related emissions dominate the composition of anthropogenic VOCs in Beijing. The spatial correlation between the emission inventory and satellite inversion result was significant ($p < 0.01$) with a correlation coefficient of 0.75. However, there were discrepancies between the relative contributions of fuel combustion, emissions of oxygenated VOCs (OVOCs), and halocarbons from the measurements and inventory. To obtain a more accurate emission inventory, we propose the investigation of the household coal consumption, the adjustment of EFs based on the latest pollution control policies, and the verification of the source profiles of OVOCs and halocarbons.

1 Introduction

Ambient volatile organic compounds (VOCs) encompass of various kinds of chemical substances that predominantly help to form the ground-level ozone (O_3) and the secondary organic aerosol (SOA) (Toro et al., 2006). Their direct emission sources include biogenic and anthropogenic sources. Most VOCs are emitted naturally on a global scale; however, in urbanized areas, they are mainly emitted anthropogenically (Guenther et al., 2012;Janssens-Maenhout et al., 2015). In addition, some VOC species have adverse effects on human health (Bari et al., 2016;Weichenthal et al., 2012). Therefore, it is essential to acquire reliable knowledge of

anthropogenic VOC emissions to develop strategies for reducing the emissions and ambient concentrations of secondary pollutants.

The emission inventory is a widely used method for calculating the emissions of VOCs, through which the magnitude, strength, spatial and temporal distribution, source structure of VOC emissions, and other related information can be provided (Wang et al., 2014). Moreover, emission inventories are important input data for the chemical transport model (Hodzic et al., 2010;Coll et al., 2010). Since the pioneering study by (Piccot et al., 1992), the "Emission factor (EF) method" has been widely used to establish emission inventories, which estimates the emissions of VOC sources by multiplying the corresponding activities and detailed EFs (Tonooka et al., 2001;Streets, 2003;Klimont et al., 2002;Ohara et al., 2007;Bo et al., 2008;Zheng et al., 2009;Wu et al., 2016;Huang et al., 2017;Janssens-Maenhout et al., 2015). The characterization and quantification of VOC emissions are highly complicated as the emission sources of VOCs exhibit complexity and diversity (Borbon et al., 2013). Although great progress has been made in the establishment of VOC emission inventories, there are still a number of limitations (Wu et al., 2016). Based on the results of the Monte Carlo simulation, the uncertainty of the VOC emission inventory was more than 100% (Bo et al., 2008). The chemical transport model simulation studies found that existing VOC emissions inventories cannot accurately assess air quality, which makes it ineffective for meeting the management needs of developing emission reduction policies (Carmichael, 2003;Coll et al., 2010;Kim et al., 2011). Thus, developing an accurate emission inventory of anthropogenic VOCs is key for effectively controlling and reducing air pollution in the future.

Emission inventories can be verified and evaluated based on the ambient measurements of VOCs or on satellite retrievals. However, the concentration of VOCs is measured after the emission undergoes physical and chemical transformations. One method for assessing regional emissions is to perform source appointments with receptor models that can calculate different sources' contributions and assess the VOC source structures, in terms of the accuracy of the emission inventories, accordingly (Gaimoz et al., 2011;Morino et al., 2011;Wang et al., 2014). In addition, the calculation of the anthropogenic emission of individual VOC species can be performed according to two indicators, (1) the emission ratios to an inert tracer (reference compound) and (2) the known emissions for the inert tracer (Borbon et al., 2013). Subsequently, the results can be used for the verification of the species-specific emissions of the EF-based inventory. Since the satellite data possess the advantage of reflecting the spatial characteristics of VOCs (Karplus et al., 2018), satellite-derived anthropogenic VOC emission estimations obtained from the chemical transport model can be utilized to evaluate the spatial distribution of the EF based emission inventories (Henne et al., 2016).

Earlier studies by various research groups applied only one of these methods to evaluate either the source structure or species-specific emissions of VOC emission inventories. Moreover, most studies have been based on the data from one or two-month ambient measurements, which cannot accurately represent the annual emissions. Also, there is a lack of systematic analysis of the qualities and uncertainties of anthropogenic VOC emission inventories. Therefore, we took the VOC emissions of the Beijing–Tianjin–Hebei (BTH) region as a case for the verification of a method for establishing an anthropogenic VOC emission inventory. The BTH region is the political center of China, a developed cluster of large cities, and one of the most polluted areas in China (Jiang et al., 2015). In recent years, severe haze events have occurred frequently in the BTH region (Zhu et al., 2016), and the mixing ratios of O_3 have increased significantly (Ma et al., 2016). There is an urgent need for effective pollution control measures in the area.

Atmos. Chem. Phys. Discuss., https://doi.org/10.5194/acp-2018-1133
Manuscript under review for journal Atmos. Chem. Phys.
Discussion started: 3 January 2019

In this study, the emission inventory of anthropogenic VOCs in 2015 in the BTH region of China was developed at a 3 km × 3 km spatial resolution based on the EF method. We conducted online measurements of ambient VOCs at an interval of 1 h in January, April, July, and October 2015 at an urban site in Beijing. We extracted the VOC emissions of the BTH region from a satellite-derived anthropogenic VOC emission inventory. The source structure, species-specific VOC emissions, and spatial distribution of the emission inventory were evaluated based on online measurements and satellite retrievals.

2 Methodology

2.1 Establishment of the anthropogenic VOC emission inventory

Through a systematic literature review, we found that the anthropogenic VOC emission inventory methodologies are similar, but the source classification and EFs used in some studies are different. So, this study combined the existing source classification system, EF databases, and source profile databases, followed by establishing the emission inventory in the BTH region (Bo et al., 2008;Wu et al., 2016;Huang et al., 2017;Zhao et al., 2017;Zhong et al., 2017). A detailed description of the method is provided below.

2.1.1 Source classification

According to the actual state of VOC emissions in the BTH region, a four-level categorization was used to classify the anthropogenic VOC sources (Wu et al., 2016). Level 1 has five sub-levels in total: transportation, the stationary combustion of fossil fuel, biomass burning, solvent utilization, and industrial processes. For example, transportation, a Level 1 source, was further divided into off-road transportation and on-road vehicles in Level 2. On-road vehicles can be divided into buses, passenger cars, motorcycles, light-duty vehicles, as well as heavy-duty vehicles in Level 3 based on the fleet type. Level 3 sources can be further divided into Level 4 sources based on fuels. Table S1 lists these classifications in detail.

2.1.2 Emission estimation and allocation

Calculation of on-road vehicular VOC emissions was performed taking into account the EFs, number of vehicles, and the corresponding average mileage for each vehicle category per year, following Eq. (1).

$$E_V = \sum P_{i,j} \times VMT_{i,j} \times EF_{i,j} \quad \text{Eq. (1)}$$

where E_v is the vehicular VOC emission (Gg); $P_{i,j}$ denotes the number of vehicles in category i under emission standard j; $VMT_{i,j}$ denotes the average mileage per year in km for vehicles in category i under emission standard j; and $EF_{i,j}$ denotes the emission factor in g km^{-1} for vehicles in category i under emission standard j. EFs were calculated by COPERT 4, a widely used software application for calculating emissions from road transport. The input parameters included the fuel information, monthly ambient temperature, average speeds and so on. The method has been explained in detail in previous studies (Cai and Xie, 2013). Furthermore, the vehicles were classified into different categories according to COPERT 4.

The Level 2 sources of biomass burning include biofuel combustion and crop field residue burning. Multiplying the activity data by corresponding EFs yields the emissions estimate of biomass burning. For crop residue burning in fields, the activity data was the total mass of crop residues burned in fields, which can be

calculated based on the crop production, the grain-to-straw ratio of each crop type, the proportion of field crop residue burning, the burning efficiency, and the proportion of dry matter in the crop residue. Li et al. (2016) described in detail the method used to obtain the activity data. The EFs of biomass burning were obtained from local experimentally measurements, as shown in Table S1.

The emission estimation of other VOC sources, including off-road transportation, the stationary combustion of fossil fuel, industrial processes, and solvent utilization, were estimated by multiplying the corresponding activities and detailed EFs. The EFs used in this study were obtained from locally measured EFs, recently published literature, national or local discharge standards, the EPA AP42 Report (*http://www3.epa.gov/ttnchie1/ap42/*) and the EEA Air Pollutant Emission Inventory Guidebook 2013. The detailed sub-sources and the EFs of each sub-source are listed in Table S1.

In the current study, selected county-level statistical data were prioritized to calculate the VOC emissions. For the sources without county-level data, either city-level or provincial-level statistical data were selected. Further, the VOC emissions estimated based on the statistical data were allocated to county-level by the most related surrogates. GDP, population, and cultivation area were used as the surrogates for allocating industrial sources, residential sources, and biomass burning sources, respectively. The county-level emissions were further divided into 3 km ×3 km grids based on a population density map (*http://www.geodoi.ac.cn/WebCn/Default.aspx*). For field crop residue burning, the allocation of emissions was carried out according to the fire counts in croplands. The MODIS Thermal Anomalies/Fire gridded level-3 product (MOD/MYD14A1) was selected to determine fire counts. The CCI-LC Map was used to identify croplands (*http://maps.elie.ucl.ac.be/CCI/viewer/index.php*). Multiplying the total VOC emission by the corresponding weight percentage from the source profile database yielded the emission of individual VOC species. The study by Wu and Xie (2017) described the source profile database used in this study in detail.

2.2 VOC sampling and analysis

The online observations of ambient VOCs were conducted at an interval of 1 h in January, April, July, and October 2015, representing winter, spring, summer, and fall, respectively. The roof of the Technical Physics Building at Peking University (PKU, 39.99 °N, 116.33 °E, Fig. 1) was selected as the sampling site. During this study, a total of 2174 valid measurements were obtained. No large industrial point sources are around to the monitoring site. This site selected represents the typical urban environment of Beijing and is far from strong direct emissions (Song et al., 2007;Li et al., 2015;Wang et al., 2015).

A custom-built online system was used to collect and analyze the ambient VOCs in a continuous and automatic manner. The system is a gas chromatography-mass spectrometry/flame ionization detector (GC-MS/FID) with a time resolution of 1 hour (*TH-PKU 300B, Wuhan Tianhong Instrument Co. Ltd., China*). A total of 104 C2-C11 VOC species (see Table S2) belonging to alkanes (27), alkenes (13), aromatics (16), halocarbons (29), alkynes (1), nitriles (1), and oxygenated VOCs (OVOCs,17) were recognized and quantified by standard gases (*source from the Environmental Technology Center, Canada, and Linde Electronic*). In addition, five concentrations of standard gases were used to perform monthly calibrations. The method detection limit (MDL) exhibited by the GC-MS/FID was in the range of 0.002 ppbv to 0.070 ppbv for each targeted species. A more detailed description of this system has been provided elsewhere (Li et al., 2015).

Atmos. Chem. Phys. Discuss., https://doi.org/10.5194/acp-2018-1133
Manuscript under review for journal Atmos. Chem. Phys.
Discussion started: 3 January 2019

2.3 Emission inventory verification system

The validation of the emission inventory was conducted based on ambient VOC measurements and satellite retrieval results. Firstly, emission strengths of VOCs on the basis of emission ratios relative to CO were estimated, and the results were compared with the emission inventory developed here to evaluate the species-specific emissions. Secondly, the positive matrix factorization (PMF) receptor model was applied to evaluate the VOC source structure with regard to its accuracy in the emission inventory. Thirdly, the study compared the emission inventory developed here with a satellite-based anthropogenic VOC emission inventory to evaluate the spatial distribution and annual VOC emissions.

2.3.1 Species VOC emissions based on ambient measurements.

Based on the ambient measurements of VOCs, the calculation of annual emissions for individual VOC species is performed based on Eq. (2):

$$E_{VOC}=E_{Ref} \times ER_{VOC} \times MW_{VOC}/MW_{Ref} \quad \text{Eq. (2)}$$

where, E_{VOC} denotes the emission of a particular VOC species per year (Gg); E_{Ref} denotes the emission of the reference compound per year (Gg); MW_{VOC} denotes the molecular weight of a particular VOC species; MW_{Ref} denotes the molecular weight of the reference compound; and ER_{VOC} denotes the emission ratio of VOC species relative to the reference compound (ppbv (ppmv Ref)$^{-1}$).

Photochemical processing is an important factor influencing the chemical compositions of VOCs in ambient air. Thus, the way in which photochemical processing impacts the measured VOC ratios should be excluded or corrected using a temporal filter (Borbon et al., 2013). The local time period 03:00 to 07:00 was set as a temporal filter to reduce the impact of photochemical processing (Wang et al., 2014). The emission ratios of VOC species to the reference compound (ER_{VOC}) from 03:00 to 07:00 local time were estimated using the liner fit model.

In this study, we selected CO as a reference compound considering that: (1) CO has similar sources as that of anthropogenic VOC and (2) CO emissions show lower uncertainty compared with VOC emissions. Thus, CO was a suitable reference compound (Coll et al., 2010;Borbon et al., 2013;Wang et al., 2014). The CO levels in the ambient air were obtained from the Wanliu National Air Quality Monitoring Station (*http://zx.bjmemc.com.cn*). The annual emission value of CO was obtained from the CO emission inventory of the MarcoPolo Project (*http://www.marcopolo-panda.eu*), which has been validated based on the chemical transport model and measurement data. The spatial resolution of this CO emission inventory is 0.25 ° × 0.25 °. To obtain reasonable results, we compared the VOC emissions of the grid where the PKU site was located (Fig. S1).

2.3.2 Source apportionments

The U.S.EPA PMF 5.0 model (U.S.EPA, 2014) was applied to the ambient VOC source apportionments. More information about the PMF model can be seen elsewhere (Paatero and Tapper, 1994), while the section below gives a brief discussion on some related concepts that enable a better understanding of the analysis in this study. Since the PMF model is a mathematical approach to quantify the contribution of sources, it is necessary to use a large number of samples to ensure the reliability of the results. During the collection period, a total of 2174 valid measurements were obtained for 104 VOC species. The PMF required two input files: (1) concentration values of sample species and (2) the uncertainty values of sample species. The observed uncertainty file was set following

the method proposed by Polissar et al. (1999). The PMF model can calculate each species' signal to noise ratio (S/N) according to the input files. Species were categorized as "Bad" when the S/N ratio was < 0.2 and "Weak" when the S/N ratio was > 0.2 but < 0.5. Two to ten factors solutions were calculated by PMF model. The most appropriate number of factors were selected by some mathematical indicators calculated following the PMF model, including the coefficient of determination, Q value, a possible explanation of the sources, and the residual distribution.

2.3.3 Satellite-derived emission inventory

To evaluate the spatial distribution of the EF based VOC emission inventory and the VOC annual emissions, we compared the emission inventory established in our study with satellite-derived anthropogenic VOC emission estimations. The satellite-derived estimations were obtained from the Global Emission project (*http://tropo.aeronomie.be/datapage_BIRA.php?species=TNMVOC*). The anthropogenic VOC emissions were derived based on source inversion with the IMAGESv2 model (Stavrakou et al., 2009) which is limited by the column densities of tropospheric HCHO from OMI satellite instrument (De Smedt et al., 2015). HCHO is a high-yield product of VOC species oxidation. Its atmospheric lifetime is relatively short (only a few hours) relative to photolysis and oxidation. Its column concentration is directly related to emissions. Therefore, satellite observations of formaldehyde column concentrations can provide a "top-down" constraint for better quantitation of high spatial-temporal resolution of VOCs. The spatial resolution of the satellite-derived emissions was 0.25 °× 0.25 °and the temporal resolution was one month. To facilitate the spatial distribution verification, the emissions of the 3 km × 3 km emission inventory established in this study were weighted and summed in the 0.25 ° × 0.25 ° grid, so that the spatial resolution was consistent with the satellite inversion emission inventory.

3 Results and discussion

3.1 VOC emission inventory in the BTH region in 2015

A total of 3277.66 Gg of anthropogenic VOC were emitted in BTH region in 2015, accounting for about 10% of the national VOC emissions (Wu et al., 2016). Emissions in the Beijing, Tianjin, and Hebei provinces were 411.72 Gg, 666.53 Gg, and 2199.41 Gg, respectively. The spatial distribution of VOC emissions is shown in Fig. 2. The emissions were lower in the northern part of the BTH region and the emission density was higher in the southeast. Moreover, the southwestern part of Beijing, the southeastern part of Tianjin, and the eastern part of Shijiazhuang displayed high VOC emissions.

Figure 3 illustrates the contribution of each source to the total VOC emissions. For the BTH region, industrial processes were the largest source, accounting for 39% of the total VOC emissions. The next was transportation with emissions of 1080.62 Gg, accounting for 33% of the total emissions. Emissions from solvent utilization, biomass burning, and fuel combustion contributed 18%, 6%, and 4 % of total VOC emissions, respectively. The primary source of VOC emissions in Beijing was transportation, while in the Tianjin and Hebei provinces it was industrial processes.

Figure 4 illustrates the chemical compositions of VOC emissions in the BTH region. The emissions of aromatics, alkanes, OVOCs, and alkenes accounted for 34%, 32%, 17%, and 11% of total anthropogenic VOC emissions, respectively. Aromatics and alkanes were the main compound groups of anthropogenic VOCs, with

annual emissions of 1412.6 Gg and 1058.6 Gg, respectively. Emissions of alkynes, halocarbons, other VOCs and nitrile were much lower, accounting for 2.2%, 2.2%, 1.4%, and 0.2% of total anthropogenic VOC emissions, respectively. The species with the highest emissions are listed in Fig. 4. The he top ten species are m/p-xylene, toluene, ethylbenzene, ethylene, n-hexane, benzene, ethane, ethanol, o-xylene, and isopentane with annual emissions of 227.0 Gg, 216.9 Gg, 154.5 Gg, 142.1 Gg, 140.8 Gg, 138.1 Gg, 113.3 Gg, 102.2 Gg, 94.7 Gg and 91.1 Gg, respectively. Among the 10 species, five belonged to aromatics, three to alkanes, one to ethene, and one to OVOCs.

3.2 Verification of species-specific VOC emissions

3.2.1 VOC mixing ratios

Figure 5 presents the average mixing ratios and chemical compositions of VOCs in January, April, July, and October 2015. The average mixing ratio of VOCs was about 49.94 ppbv in 2015, varying from 10.67 ppbv to 245.54 ppbv. The highest VOC mixing ratio was occurred in January, with an average value of 62.26 ppbv. The VOC mixing ratios were relatively lower in April and July, with average values of 41.09 ppbv and 41.77 ppbv, respectively. In October, the average mixing ratio of VOCs was 50.64 ppbv. The VOCs species varied dramatically across the four seasons. Overall, alkanes dominated total VOCs during all seasons, accounting for 31.2%–39.5% on average. In January, alkanes constituted the largest group of VOCs (39.5%), and the next one was alkenes (22.6%). In other months, the highest VOC group was also alkanes, followed by OVOCs.

Figure 6 presents the time series of VOC mixing ratios. The mixing ratios of VOCs in January were variable, with maximum value of 245.54 ppbv. There were lots of periods with high VOC mixing ratios in January. In April, the average VOC mixing ratio was not as high as in January but the mixing ratios of VOCs change a lot, a maximum value of 150.24 ppbv. The mixing ratios of VOCs in July were stable, with the highest level of 92.28 ppbv. The VOCs accumulated in early October decreased sharply in the middle of the month, then began to accumulate again with the change of the diffusion condition. The highest VOC mixing ratio in October was 201.10 ppbv.

The VOC species showing the highest mixing ratios in January, April, July, and October (top 20) are listed in Table 1. Ethane exhibited the largest proportion during all the four months. Ethene, acetylene, propene, and benzene are considered typical combustion tracers (Liu et al., 2008). Compared with the other months, the mixing ratios of combustion sources tracers were much higher in January. Benzene and toluene were important VOC species. During combustion processing, the emissions of benzene are much higher than toluene. As shown in Table 1, benzene showed a higher mixing ratio than toluene in January. In contrast, the benzene showed a lower mixing ratio compared with toluene in the other three months. Combustion may be an important source in winter. During July, the levels of acetone, methyl methacrylate, and 2-butanone were much higher, which may be influenced by secondary formation process. The mixing ratios of n-butane and i-pentane were also very high in July, which may be influenced by the evaporation of gasoline in summer.

3.2.2 Verification of individual VOC species emissions

Here, we selected CO as a reference compound for anthropogenic VOC species. For verifying the rationale of setting CO as the reference compound, this study analyzed the mutual influence of mixing ratios of individual

VOC species and CO levels. All VOC species, except β-pinene and $C_2F_3Cl_3$, were significantly related to CO ($p < 0.05$). Acetylene, ethane, and ethene were the most obviously related to CO ($r > 0.8$), and benzene, propene, tran-2- butane, 2,3-dimethyl butane, and i-butane also displayed strong correlations with CO ($r > 0.6$). The correlation coefficients between some halocarbons/ketones and CO were lower as halocarbons and ketones have a few different emission sources from CO.

Table S2 listed the emission ratios for individual VOC species measured in this study and compared the individual emissions estimated from the emission ratios and emission inventory. Based on the annual emissions derived from the measurements, the top fifteen species with the highest emissions were ethane, ethene, propane, acetylene, acetone, toluene, dichloromethane, n-butane, benzene, methyl methacrylate, ethyl acetate, propene, i-pentane, i-butane, and 2-butanone. Based on the annual emissions derived from the emission inventory, the top fifteen species with higher emissions were m-/p-xylene, toluene, ethylbenzene, benzene, ethylene, o-xylene, i-pentane, ethane, tetrachloroethylene, ethyl acetate, 1,2, 4-trimethylbenzene, propylene, pentane, n-butane, and n-hexane.

The emissions of individual VOC species determined by the measurements and emission inventory for the sampling site in 2015 were displayed in Fig. 7. After the comparison with results obtained from measurements, the emissions for a majority of the non-methane hydrocarbon (NMHC) species were agreed within ±100% in the emission inventory. The emissions for acetonitrile came from the two methods were similar, however, the annual emissions of many OVOCs and halocarbons were much lower in the emission inventory than that in the measurements results. Moreover, the emission levels of some aromatics in the emission inventory were higher than that of the measurements.

Figure 8 makes a direct comparison between the emissions of individual VOC species from the measurements and emission inventory. The annual emissions for alkanes were in agreement between the two methods, except ethane and propane, which are important tracers of natural gas and LPG (Katzenstein et al., 2003). The emission inventory may underestimate the VOC emissions from the utilization of natural gas and LPG. This conclusion was consistent with the study by Wang et al. (2014), which compared the emission ratios of 27 sites in Beijing to the INTEX-B emission inventory.

The annual emissions for the alkenes, except ethene, correlated well. The acetylene in the emission inventory showed a lower annual emission compared with that from the measurements. Ethene and acetylene are mainly emitted through an incomplete combustion process. The lower emissions of the two species in the emission inventory indicated that the emission inventory might have underestimated the VOC emissions from combustion sources. Emissions of some aromatics like toluene, o-xylene, and m/p-xylene in the emission inventory were higher compared with that from the measurements. Toluene and xylene were mainly emitted from various solvent utilization sources, such as automobile coatings, building coatings, and furniture manufacturing. The common character of these sources is that Beijing had issued local VOC emission standards for the above sources since 2015. The enactment of local VOC emission standards decreases the emission of some aromatics. However, the influence of those standards on EFs has not been considered before, which might lead to higher emissions of toluene, o-xylene, and m/p-xylene in the emission inventory than in measurements.

OVOC and halocarbons showed a much lower emission in the emission inventory compared with that from the observations, which might be due to the lack of reliable source profiles. The VOC source profiles obtained from the local measurements mainly focused on the monitoring of NMHC species, and fewer studies have been

conducted on the measurement of OVOCs and halocarbons (Mo et al., 2016). Moreover, the extensively used VOC source profiles database, USEPA SPECIATE, excludes VOC species with very low atmospheric photochemical reactions, such as methylene chloride, methyl chloroform, and fluorochemicals (USEPA SPECIATED). For instance, both acetone and 2-butanone are carbonyl compounds. Vehicle exhaust, biomass combustion, food flue gas, surface coating, and industrial exhaust gas are the sources of carbonyl compounds, while only 45 of the more than 150 sources profiles included acetone and 38 source profiles contained 2-butanone. Another example is that of esters, which are used as tracers of industrial emissions and are emitted by most of the industrial processes and surface coating processes. However, only 12 sources in the source profile database contained methyl acetate, 6 sources contained methyl methacrylate, 29 sources contained ethyl acetate, and 14 sources contained butyl acetate. Halocarbons are also vital tracers of industrial sources. Of all the source profile databases collected in this study, only 33 sources profiles contained methyl chloride, 28 sources contained chloroform, 35 sources contained 1,2-dichloroethane, and 26 sources contained 1,2-dichloropropane. Consequently, more source emission monitoring investigations need to be carried out to obtain reliable source profiles of VOC emissions.

3.3 Verification of source structures

3.3.1 Source appointments

The PMF receptor model was used to conduct dynamic source apportionment according to the measured VOCs. The following analysis adopted 63 strong and 5 weak species, accounting for more than 90% of the total VOC mixing ratios. In the following, six sources were identified, including (1) vehicle-related sources, (2) fuel combustion, (3) aged air mass and biomass burning, (4) industrial processes, (5) biogenic source, (6) solvent utilization. Figure 9 shows the source profiles of individual sources, and the source identification is described in the supplemental file.

Figure 10 illustrates source contribution percentages in January, April, July, and October. In January, fuel combustion made the largest contribution (55%) to VOC mixing ratios. Emissions from vehicle–related source and industrial processes contributed 19%, and 14% to total VOC mixing ratios, respectively. The contributions from aged air mass, solvent utilization, and biogenic were relatively low at 7%, 3%, and 1%, respectively. In April, aged air mass made the largest contribution (33%) to VOCs, followed by vehicle-related sources (22%) and industrial processes (21%).The contribution proportion of fuel combustion, solvent utilization, and biogenic respectively was 12%, 7%, and 5% of the total VOC mixing ratios. In July, vehicle-related sources accounted for 50% the total VOCs. Meanwhile, the biogenic source elevated from 5% in April to 18% in July. Emissions from solvent utilization, aged air mass, industrial processes, and fuel combustion respectively contributed 12%, 10%, 6%, and 4% of total VOCs. In October, vehicle-related sources were also the most important source, accounting for 33% of the total VOC mixing ratios, followed by solvent utilization (23%), aged air mass (18%), and industrial processes (16%). Contributions from fuel combustion and biogenic sources were relatively low, with values of 6% and 5%, respectively.

3.3.2 Comparison between the emission inventory and PMF results

This study compared the annual average PMF results with the VOC source structures of the emission inventory

established (Fig. 11). The results of PMF demonstrated that transportation made the largest contribution to VOCs, which accounted for 36% of the total anthropogenic VOC emissions. On the other hand, the results of the emission inventory also showed that transportation was the largest contributor to VOCs (33 %). The contribution of industrial processes (20%) from PMF results was comparable with the result from emission inventory (30%). The contribution for the solvent utilization obtained from the PMF result was 19%, which was higher than the value of the emission inventory (30%). The relative contribution of the fuel combustion source from the PMF result was 25%, which was significantly lower than that in the emission inventory (8%).

According to the PMF results and the emission inventory, the vehicle-related emissions were the primary source in urban area in Beijing. Solvent utilization and industrial processes also contributed significantly. However, large differences were observed in the stationary combustion of fossil fuel consistent with the comparison results shown in section 3.2.2.

According to the seasonal PMF result (Fig. 10), the relative contribution of fuel combustion in winter was 55%, significantly higher than the contributions in the spring (12%), summer (4%), and fall (6%). However, the relative contributions of fuel combustion in the spring, summer, and fall were similar to the value obtained from the emission inventory. Therefore, the difference between the contributions of PMF and the emission inventory may be caused by the large difference of the contributions in winter.

On the basis of the above comparisons of the VOC source structure, we inferred that: (1) the contributions of the vehicles, solvent utilization, and industrial processes from the emission inventory and the PMF results were similar; and (2) the fuel combustion in the emission inventory showed a considerably lower relative contribution than the value from the PMF analysis in winter, the central heating season in Beijing. The emission inventory was established by multiplying statistical data and EFs. Table S1 lists the EFs of fossil fuel combustion sources used here, which were referenced from local measurement studies and were comparable with EFs reported by the US government or the European Union (USEPA, 1995; EEA, 2013). Hence, we attributed the large difference between fuel combustion contributions from the PMF analysis and emission inventory to the uncertainties of activity data obtained from statistical information. For industrial-related activity data, the statistical data was relatively reliable; however, uncertainty in the statistical data was very high for residential-related activity data. For instance, it is very difficult to quantify the consumption of coal briquettes and chunks, the major fossil fuel for heating and cooking in Chinese households, since such coal for household often goes unreported in official statistics (Liu et al., 2016) Moreover, it is suspected that actual residential coal consumption is much higher than it reported in official statistics (Andersson et al., 2015). We speculate that the underestimation of the emissions from stationary combustion of fossil fuel by the emission inventory can be explained by the incomplete statistical data of residential coal consumption. In future studies, it is necessary to estimate the exact activity data and emissions of residential fossil fuel combustion through scientific approaches.

3.4 Verification of spatial distributions

The satellite-derived emission inventory revealed that the VOC emissions in the BTH region were 4368.50 Gg, while the annual emissions according to the EF-based emission inventory were 3277.66 Gg. The deviation of the emissions calculated by the two methods is 30%, within a reasonable error range. The two types of emission inventory shown similar distributions (Fig. 12a) and comparable emissions (Figure 13.a) for the gridded emissions. The spatial distributions of VOC emissions derived from the emission inventory and satellite data are shown in

Fig. 13. The gridded VOC emissions of the emission inventory displayed significant correlations with the emissions derived from the satellite ($p < 0.05$), with a correlation coefficient of 0.75. The areas with higher and lower VOC emissions in the two emission inventories are also consistent. The areas with higher emissions were concentrated in the urban areas of Beijing and Tianjin, whereas areas with lower emissions were concentrated in the north of the BTH region, including Zhangjiakou and Chengde. The emissions of EF-based emission inventory present some positive biases compared to the satellite-derived emissions for the grids located in the south (Fig. 12b). The emissions calculated by the EF-based emission inventory were higher than those calculated by the satellite-derived emission inventory for Xingtai and Handan (Fig. 13), two heavy industrial cities in Hebei province.

The temporal resolution of the satellite-derived emission inventory is one month. As shown in Fig. 14, monthly variations of VOC emissions exhibit obvious seasonal characteristics, with maximum in winter and minimum in summer, which are consistent with the seasonal characteristics of the ambient VOC mixing ratios (Fig. 5). However, monthly profiles for EF-based emission inventories, which usually developed based on monthly statistics, didn't exhibit seasonal variations (Li et al., 2017). The satellite-derived emission inventories can better reflect the monthly characteristics of VOC emissions and be used to allocate monthly emissions.

The satellite-derived emission inventory possesses the advantage of efficiently reflecting the spatial and monthly characteristics of the VOC emissions(Geng et al., 2017). The significant correlation between the emission inventory established here and the satellite-derived emission inventory is indicative of the reliability of the spatial allocation method and the spatial emissions of the emission inventory. The satellite-derived emission inventory can provide constrains to improve the existing understanding of monthly profiles of VOC emissions.

4 Conclusions

An emission inventory of anthropogenic VOCs was established for the BTH region in China at a 3 km × 3 km spatial resolution based on the EF method. We conducted VOC online observations selecting a site in the urban area of Beijing. Based on the measurements, we estimated the annual emission strengths of VOCs according to their emission ratios relative to CO, then compared these results with the emission inventory established in this study to verify the species-specific VOC emissions. The PMF model was used to qualify the relative contribution made by each source. The result was compared with the emission inventory to evaluate the source structure of the VOCs. We also compared the emission inventory established in our study with a satellite-derived anthropogenic VOC emission inventory for verification of the spatial distribution and VOCs annual emissions.

According to the PMF results and the emission inventory, the vehicle-related emissions dominate the composition of anthropogenic VOCs in Beijing. The annual emissions of NMHCs derived from the measurements were consistent with the results of the emission inventory. The total amount of anthropogenic VOC emissions of the emission inventory was similar to the satellite inversion result, with a deviation of 30%. The spatial correlation between the emission inventory and the satellite inversion result was significant ($p < 0.01$) with a correlation coefficient of 0.75.

Our results showed that the vehicle-related VOC emissions estimated by the emission inventory based on the EF method were reliable. The emissions of NMHCs estimated by the emission inventory were accurate and the method of spatial distribution was feasible. Nevertheless, there are a few limitations of the existing method for

415 establishing an anthropogenic VOC emission inventory based on EFs. Firstly, there is a large difference between the relative contributions of fuel combustion, and the method underestimated the emissions from fuel combustion sources in winter. Secondly, the emissions of OVOCs and halocarbons estimated in the emission inventory appeared much lower than those derived from the measurements due to the lack of reliable source profiles. Thirdly, emissions of some aromatics estimated in the emission inventory were higher than the values derived from the
420 measurements due to the enactment of some local emission standards.

To acquire a more accurate VOC emission inventory, we propose the following improvements to the future emission inventories: (1) the investigation of household coal consumption to improve the accuracy of activity data; (2) the adjustment of EFs based on the latest pollution control policies to establish dynamic emissions inventories; and (3) the verification of OVOCs and halocarbons emissions and (4) the performance of more source emission
425 monitoring studies to obtain reliable source profiles of VOC emissions.

Author contributions.

SDX designed the study, JL performed the data analysis and wrote the paper. YFH contributed to the online measurements. MS contributed to the development of the emission inventory. YQS and ZYX assisted with data collection. All authors assisted with interpretation of the results and the writing of the paper.

430 **Competing interests.**

The authors declare that they have no conflict of interest.

Acknowledgements.

This work was supported by the National Natural Science Foundation of China for "The development and validation of emission inventories of anthropogenic volatile organic compounds in the Beijing−Tianjin−Hebei
435 region, China" (Grants No. 91544106), and by the National Air Pollution Prevention Joint Research Center of China for "The research of characteristics, emission reduction and regulatory system of volatile organic compounds in key sectors" (Grants No. DQGG0204).

References

Andersson, A., Deng, J., Du, K., Zheng, M., Yan, C., Sköld, M., and Gustafsson, Ö.: Regionally-Varying
440 Combustion Sources of the January 2013 Severe Haze Events over Eastern China, Environ Sci Technol, 49, 2038-2043, 10.1021/es503855e, 2015.

Bari, M. A., Kindzierski, W. B., and Spink, D.: Twelve-year trends in ambient concentrations of volatile organic compounds in a community of the Alberta Oil Sands Region, Canada, Environ Int, 91, 40-50, 10.1016/j.envint.2016.02.015, 2016.

445 Bo, Y., Cai, H., and Xie, S. D.: Spatial and temporal variation of historical anthropogenic NMVOCs emission inventories in China, Atmospheric Chemistry And Physics, 8, 7297-7316, 2008.

Borbon, A., Gilman, J. B., Kuster, W. C., Grand, N., Chevaillier, S., Colomb, A., Dolgorouky, C., Gros, V., Lopez, M., Sarda-Esteve, R., Holloway, J., Stutz, J., Petetin, H., McKeen, S., Beekmann, M., Warneke, C., Parrish, D. D., and de Gouw, J. A.: Emission ratios of anthropogenic volatile organic compounds in northern mid-
450 latitude megacities: Observations versus emission inventories in Los Angeles and Paris, Journal of Geophysical Research: Atmospheres, 118, 2041-2057, 10.1002/jgrd.50059, 2013.

Cai, H., and Xie, S.: Temporal and spatial variation in recent vehicular emission inventories in China based on dynamic emission factors, J Air Waste Manage, 63, 310-326, 10.1080/10962247.2012.755138, 2013.

Carmichael, G. R.: Regional-scale chemical transport modeling in support of the analysis of observations obtained during the TRACE-P experiment, J Geophys Res, 108, 10.1029/2002jd003117, 2003.

Coll, I., Rousseau, C., Barletta, B., Meinardi, S., and Blake, D. R.: Evaluation of an urban NMHC emission inventory by measurements and impact on CTM results, Atmos Environ, 44, 3843-3855, 10.1016/j.atmosenv.2010.05.042, 2010.

De Smedt, I., Stavrakou, T., Hendrick, F., Danckaert, T., Vlemmix, T., Pinardi, G., Theys, N., Lerot, C., Gielen, C., Vigouroux, C., Hermans, C., Fayt, C., Veefkind, P., Müller, J. F., and Van Roozendael, M.: Diurnal, seasonal and long-term variations of global formaldehyde columns inferred from combined OMI and GOME-2 observations, Atmospheric Chemistry and Physics, 15, 12519-12545, 10.5194/acp-15-12519-2015, 2015.

EEA, Air Pollutant Emission Inventory Guidebook. EEA technical Report No. 12, 2013 EP and CEU, 2013.

Gaimoz, C., Sauvage, S., Gros, V., Herrmann, F., Williams, J., Locoge, N., Perrussel, O., Bonsang, B., d'Argouges, O., Sarda-Esteve, R., and Sciare, J.: Volatile organic compounds sources in Paris in spring 2007. Part II: source apportionment using positive matrix factorisation, Environmental Chemistry, 8, 91-103, 10.1071/en10067, 2011.

Geng, G., Zhang, Q., Martin, R. V., Lin, J., Huo, H., Zheng, B., Wang, S., and He, K.: Impact of spatial proxies on the representation of bottom-up emission inventories: A satellite-based analysis, Atmospheric Chemistry and Physics, 17, 4131-4145, 10.5194/acp-17-4131-2017, 2017.

Guenther, A. B., Jiang, X., Heald, C. L., Sakulyanontvittaya, T., Duhl, T., Emmons, L. K., and Wang, X.: The Model of Emissions of Gases and Aerosols from Nature version 2.1 (MEGAN2.1): an extended and updated framework for modeling biogenic emissions, Geoscientific Model Development, 5, 1471-1492, 10.5194/gmd-5-1471-2012, 2012.

Henne, S., Brunner, D., Oney, B., Leuenberger, M., Eugster, W., Bamberger, I., Meinhardt, F., Steinbacher, M., and Emmenegger, L.: Validation of the Swiss methane emission inventory by atmospheric observations and inverse modelling, Atmospheric Chemistry and Physics, 16, 3683-3710, 10.5194/acp-16-3683-2016, 2016.

Hodzic, A., Jimenez, J. L., Madronich, S., Canagaratna, M. R., DeCarlo, P. F., Kleinman, L., and Fast, J.: Modeling organic aerosols in a megacity: potential contribution of semi-volatile and intermediate volatility primary organic compounds to secondary organic aerosol formation, Atmospheric Chemistry and Physics, 10, 5491-5514, 10.5194/acp-10-5491-2010, 2010.

Huang, G., Brook, R., Crippa, M., Janssens-Maenhout, G., Schieberle, C., Dore, C., Guizzardi, D., Muntean, M., Schaaf, E., and Friedrich, R.: Speciation of anthropogenic emissions of non-methane volatile organic compounds: a global gridded data set for 1970–2012, Atmospheric Chemistry and Physics, 17, 7683-7701, 10.5194/acp-17-7683-2017, 2017.

Janssens-Maenhout, G., Crippa, M., Guizzardi, D., Dentener, F., Muntean, M., Pouliot, G., Keating, T., Zhang, Q., Kurokawa, J., Wankmüller, R., Denier van der Gon, H., Kuenen, J. J. P., Klimont, Z., Frost, G., Darras, S., Koffi, B., and Li, M.: HTAP_v2.2: a mosaic of regional and global emission grid maps for 2008 and 2010 to study hemispheric transport of air pollution, Atmospheric Chemistry and Physics, 15, 11411-11432, 10.5194/acp-15-11411-2015, 2015.

Jiang, C., Wang, H., Zhao, T., Li, T., and Che, H.: Modeling study of PM_{2.5} pollutant transport across cities in China's Jing–Jin–Ji region during a severe haze episode in December 2013, Atmospheric Chemistry and Physics, 15, 5803-5814, 10.5194/acp-15-5803-2015, 2015.

Karplus, V. J., Zhang, S., and Almond, D.: Quantifying coal power plant responses to tighter SO2 emissions standards in China, Natl. Acad. Sci. U. S. A., 115, 7004-7009, 10.1073/pnas.1800605115, 2018.

Katzenstein, A. S., Doezema, L. A., Simpson, I. J., Balke, D. R., and Rowland, F. S.: Extensive regional atmospheric hydrocarbon pollution in the southwestern United States, Proc. Natl. Acad. Sci. U. S. A., 100, 11975-11979, 10.1073/pnas.1635258100, 2003.

Kim, S. W., McKeen, S. A., Frost, G. J., Lee, S. H., Trainer, M., Richter, A., Angevine, W. M., Atlas, E., Bianco, L., Boersma, K. F., Brioude, J., Burrows, J. P., de Gouw, J., Fried, A., Gleason, J., Hilboll, A., Mellqvist, J., Peischl, J., Richter, D., Rivera, C., Ryerson, T., Hekkert, S. T. L., Walega, J., Warneke, C., Weibring, P., and Williams, E.: Evaluations of NOx and highly reactive VOC emission inventories in Texas and their implications for ozone plume simulations during the Texas Air Quality Study 2006, Atmospheric Chemistry And Physics, 11, 11361-11386, 10.5194/acp-11-11361-2011, 2011.

Klimont, Z., Streets, D. G., Gupta, S., Cofala, J., Fu, L. X., and Ichikawa, Y.: Anthropogenic emissions of non-methane volatile organic compounds in China, Atmos Environ, 36, 1309-1322, 10.1016/s1352-2310(01)00529-5, 2002.

Li, J., Xie, S. D., Zeng, L. M., Li, L. Y., Li, Y. Q., and Wu, R. R.: Characterization of ambient volatile organic compounds and their sources in Beijing, before, during, and after Asia-Pacific Economic Cooperation China

2014, Atmospheric Chemistry and Physics, 15, 7945-7959, 10.5194/acp-15-7945-2015, 2015.

Li, J., Li, Y., Bo, Y., and Xie, S.: High-resolution historical emission inventories of crop residue burning in fields in China for the period 1990–2013, Atmos Environ, 138, 152-161, 10.1016/j.atmosenv.2016.05.002, 2016.

Li, M., Zhang, Q., Kurokawa, J.-i., Woo, J.-H., He, K., Lu, Z., Ohara, T., Song, Y., Streets, D. G., Carmichael, G. R., Cheng, Y., Hong, C., Huo, H., Jiang, X., Kang, S., Liu, F., Su, H., and Zheng, B.: MIX: a mosaic Asian anthropogenic emission inventory under the international collaboration framework of the MICS-Asia and HTAP, Atmospheric Chemistry and Physics, 17, 935-963, 10.5194/acp-17-935-2017, 2017.

Liu, J., Mauzerall, D. L., Chen, Q., Zhang, Q., Song, Y., Peng, W., Klimont, Z., Qiu, X., Zhang, S., Hu, M., Lin, W., Smith, K. R., and Zhu, T.: Air pollutant emissions from Chinese households: A major and underappreciated ambient pollution source, Natl. Acad. Sci. U. S. A., 10.1073/pnas.1604537113, 2016.

Liu, Y., Shao, M., Fu, L. L., Lu, S. H., Zeng, L. M., and Tang, D. G.: Source profiles of volatile organic compounds (VOCs) measured in China: Part I, Atmos Environ, 42, 6247-6260, 10.1016/j.atmosenv.2008.01.070, 2008.

Ma, Z., Xu, J., Quan, W., Zhang, Z., Lin, W., and Xu, X.: Significant increase of surface ozone at a rural site, north of eastern China, Atmospheric Chemistry and Physics, 16, 3969-3977, 10.5194/acp-16-3969-2016, 2016.

Mo, Z., Shao, M., and Lu, S.: Compilation of a source profile database for hydrocarbon and OVOC emissions in China, Atmos Environ, 143, 209-217, 10.1016/j.atmosenv.2016.08.025, 2016.

Morino, Y., Ohara, T., Yokouchi, Y., and Ooki, A.: Comprehensive source apportionment of volatile organic compounds using observational data, two receptor models, and an emission inventory in Tokyo metropolitan area, J Geophys Res, 116, 10.1029/2010jd014762, 2011.

Ohara, T., Akimoto, H., Kurokawa, J., Horii, N., Yamaji, K., Yan, X., and Hayasaka, T.: An Asian emission inventory of anthropogenic emission sources for the period 1980-2020, Atmospheric Chemistry And Physics, 7, 4419-4444, 2007.

Piccot, S. D., Watson, J. J., and Jones, J. W.: A GLOBAL INVENTORY OF VOLATILE ORGANIC-COMPOUND EMISSIONS FROM ANTHROPOGENIC SOURCES, Journal Of Geophysical Research-Atmospheres, 97, 9897-9912, 1992.

Polissar, A. V., Hopke, P. K., Paatero, P., Kaufmann, Y. J., Hall, D. K., Bodhaine, B. A., Dutton, E. G., and Harris, J. M.: The aerosol at Barrow, Alaska: long-term trends and source locations, Atmos Environ, 33, 2441-2458, 10.1016/s1352-2310(98)00423-3, 1999.

Song, Y., Shao, M., Liu, Y., Lu, S. H., Kuster, W., Goldan, P., and Xie, S. D.: Source apportionment of ambient volatile organic compounds in Beijing, Environ Sci Technol, 41, 4348-4353, 10.1021/es0625982, 2007.

Stavrakou, T., Muller, J. F., De Smedt, I., Van Roozendael, M., van der Werf, G. R., Giglio, L., and Guenther, A.: Evaluating the performance of pyrogenic and biogenic emission inventories against one decade of space-based formaldehyde columns, Atmospheric Chemistry And Physics, 9, 1037-1060, 2009.

Streets, D. G.: An inventory of gaseous and primary aerosol emissions in Asia in the year 2000, J Geophys Res, 108, 10.1029/2002jd003093, 2003.

Tonooka, Y., Kannari, A., Higashino, H., and Murano, K.: NMVOCs and CO emission inventory in East Asia, Water Air Soil Poll, 130, 199-204, 10.1023/a:1013890513856, 2001.

Toro, M. V., Cremades, L. V., and Calbo, J.: Relationship between VOC and NOx emissions and chemical production of tropospheric ozone in the Aburra Valley (Colombia), Chemosphere, 65, 881-888, 10.1016/j.chemosphere.2006.03.013, 2006.

U.S. Environmental Protection Agency (USEPA): Compilation of air pollutant emission factors (AP42), Fifth Edition, Chapter 1–13, 1995.

U.S. Environmental Protection Agency (USEPA): Positive Matrix Factorization (PMF) 5.0 Fundamentals and User Guide. US Environmental Protection Agency, Office of Research and Development, Washington, D.C, 2014.

U.S. Environmental Protection Agency (USEPA): SPECIATE Version 4.4; U.S. Environmental Protection Agency: Washington, DC, February 2014.

Wang, M., Shao, M., Chen, W., Yuan, B., Lu, S., Zhang, Q., Zeng, L., and Wang, Q.: A temporally and spatially resolved validation of emission inventories by measurements of ambient volatile organic compounds in Beijing, China, Atmospheric Chemistry and Physics, 14, 5871-5891, 10.5194/acp-14-5871-2014, 2014.

Wang, M., Shao, M., Chen, W., Lu, S., Liu, Y., Yuan, B., Zhang, Q., Zhang, Q., Chang, C. C., Wang, B., Zeng, L., Hu, M., Yang, Y., and Li, Y.: Trends of non-methane hydrocarbons (NMHC) emissions in Beijing during 2002–2013, Atmospheric Chemistry and Physics, 15, 1489-1502, 10.5194/acp-15-1489-2015, 2015.

Weichenthal, S., Kulka, R., Belisle, P., Joseph, L., Dubeau, A., Martin, C., Wang, D., and Dales, R.: Personal exposure to specific volatile organic compounds and acute changes in lung function and heart rate variability among urban cyclists, Environ Res, 118, 118-123, 10.1016/j.envres.2012.06.005, 2012.

Wu, R., Bo, Y., Li, J., Li, L., Li, Y., and Xie, S.: Method to establish the emission inventory of anthropogenic volatile organic compounds in China and its application in the period 2008–2012, Atmos Environ, 127, 244-

254, 10.1016/j.atmosenv.2015.12.015, 2016.

Wu, R., and Xie, S.: Spatial Distribution of Ozone Formation in China Derived from Emissions of Speciated Volatile Organic Compounds, Environ Sci Technol, 51, 2574-2583, 10.1021/acs.est.6b03634, 2017.

Zhao, Y., Mao, P., Zhou, Y., Yang, Y., Zhang, J., Wang, S., Dong, Y., Xie, F., Yu, Y., and Li, W.: Improved provincial emission inventory and speciation profiles of anthropogenic non-methane volatile organic compounds: a case study for Jiangsu, China, Atmospheric Chemistry and Physics, 17, 7733-7756, 10.5194/acp-17-7733-2017, 2017.

Zheng, J., Shao, M., Che, W., Zhang, L., Zhong, L., Zhang, Y., and Streets, D.: Speciated VOC Emission Inventory and Spatial Patterns of Ozone Formation Potential in the Pearl River Delta, China, Environ Sci Technol, 43, 8580-8586, 10.1021/es901688e, 2009.

Zhong, Z., Sha, Q., Zheng, J., Yuan, Z., Gao, Z., Ou, J., Zheng, Z., Li, C., and Huang, Z.: Sector-based VOCs emission factors and source profiles for the surface coating industry in the Pearl River Delta region of China, Sci Total Environ, 583, 19-28, 10.1016/j.scitotenv.2016.12.172, 2017.

Zhu, X. W., Tang, G. Q., Hu, B., Wang, L. L., Xin, J. Y., Zhang, J. K., Liu, Z. R., Munkel, C., and Wang, Y. S.: Regional pollution and its formation mechanism over North China Plain: A case study with ceilometer observations and model simulations, Journal Of Geophysical Research-Atmospheres, 121, 14574-14588, 10.1002/2016jd025730, 2016.

Figure and Table captions:

590 **Table 1. The VOC species showing the highest mixing ratios (ppbv) in January, April, July, and October 2015 (top 20).**

Figure 1. The location of the BTH region in China (shaded area) and the sampling site (black dot).

Figure 2. The spatial distribution of VOC emissions in the BTH region at a 3 km × 3 km resolution.

Figure 3. Source contributions to the total VOC emission in the Beijing, Tianjin, Hebei provinces (a) and the BTH region (b), China.

595 **Figure 4. VOC emissions in the BTH region, China.**

Figure 5. Mixing ratios and compositions of VOCs (ppbv) measured at the PKU site during the four seasons and throughout the study period.

Figure 6. Time series of mixing ratios of VOCs in January, April, July, and October 2015.

Figure 7. Comparisons of VOC annual emissions (ton) derived from the ambient measures and emission inventory for
600 **the PKU site (0.25 ° × 0.25 °grid).**

Figure 8. Comparisons of individual species emissions (ton) derived from the ambient measures and emission inventory for the PKU site (0.25 ° × 0.25 °grid).

Figure 9.Source profiles for VOCs in the PKU site calculated by PMF (bars: mixing ratio of species; dots: % of species).

Figure 10.Relative contributions (%) of the six sources identified by PMF analysis in January, April, July, and October
605 **of 2015.**

Figure 11. Comparison of VOC source structure in the emission inventory (left) and the PMF results (right).

Figure 12. Comparisons between the emissions from the EF-derived emission inventory and the satellite-derived emission inventory.

Figure 13. Comparision between spatial distribution of VOC emissions obtained from the EF-derived emission
610 **inventory and the satellite-derived emission inventory with a 0.25 ° × 0.25 °spatial resolution.**

Figure 14. Monthly profiles of VOC emissions from the satellite-derived emission inventory.

Atmos. Chem. Phys. Discuss., https://doi.org/10.5194/acp-2018-1133
Manuscript under review for journal Atmos. Chem. Phys.
Discussion started: 3 January 2019

Atmospheric Chemistry and Physics Discussions

Table 1. The VOC species showing the highest mixing ratios (ppbv) in January, April, July, and October 2015 (top 20).

January		April		July		October	
Ethane	11.66	Ethane	5.67	Ethane	4.18	Ethane	5.63
Ethene	10.70	Acetone	5.53	Acetone	4.18	Propane	4.54
Acetylene	6.98	Propane	3.49	Methylmethacrylate	3.75	Acetone	4.42
Propane	5.48	Ethene	2.58	Propane	2.98	Ethene	3.73
CF2Cl2	2.58	Acetylene	2.41	Acetylene	2.47	Acetylene	3.09
Propene	2.45	Dichloromethane	2.34	Dichloromethane	2.04	Dichloromethane	2.41
n-Butane	2.10	n-Butane	1.29	Ethene	1.82	n-Butane	1.95
Acetone	1.82	Ethyl acetate	1.13	Toluene	1.55	methylmethacrylate	1.89
i-Butane	1.45	Toluene	1.06	n-Butane	1.54	Toluene	1.66
Benzene	1.30	2-Butanone	1.04	2-Butanone	1.00	Chloroform	1.40
Toluene	1.28	Chloromethane	1.03	i-Penpane	1.00	Chloromethane	1.40
i-Penpane	1.13	i-Penpane	0.88	i-Butane	0.86	i-Penpane	1.39
Dichloromethane	1.12	i-Butane	0.87	Benzene	0.80	i-Butane	1.10
2-Butanone	0.95	methylmethacrylate	0.85	1,2- Dichloroethane	0.78	Ethyl acetate	1.03
Ethyl acetate	0.89	Chloroform	0.78	Chloromethane	0.76	Benzene	1.01
Chloromethane	0.81	Benzene	0.76	Chloroform	0.66	Propene	0.87
Penpane	0.68	Penpane	0.59	Acetonitrile	0.61	Penpane	0.82
Methylmethacrylate	0.53	Propene	0.57	1,1,2,2-	0.57	n-Hexane	0.74
Butyl acetate	0.49	Acetonitrile	0.5	Penpane	0.5	1,2-	0.6
n-Hexane	0.44	Menthyl acetate	0.48	1,2-	0.49	1,2-Dichloroethane	0.59

615

Atmos. Chem. Phys. Discuss., https://doi.org/10.5194/acp-2018-1133
Manuscript under review for journal Atmos. Chem. Phys.
Discussion started: 3 January 2019

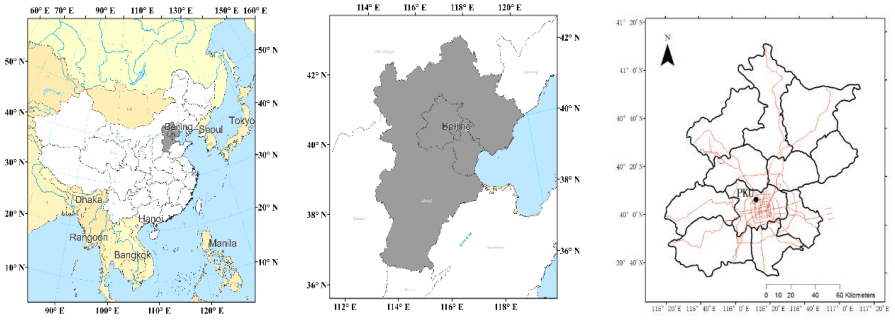

Figure 1. The location of the BTH region in China (shaded area) and the sampling site (black dot).

Atmos. Chem. Phys. Discuss., https://doi.org/10.5194/acp-2018-1133
Manuscript under review for journal Atmos. Chem. Phys.
Discussion started: 3 January 2019

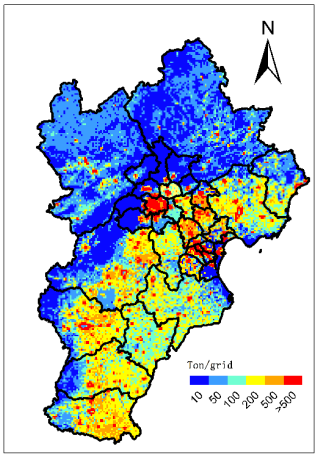

620

Figure 2. The spatial distribution of VOC emissions in the BTH region at a 3 km × 3 km resolution.

Atmos. Chem. Phys. Discuss., https://doi.org/10.5194/acp-2018-1133
Manuscript under review for journal Atmos. Chem. Phys.
Discussion started: 3 January 2019

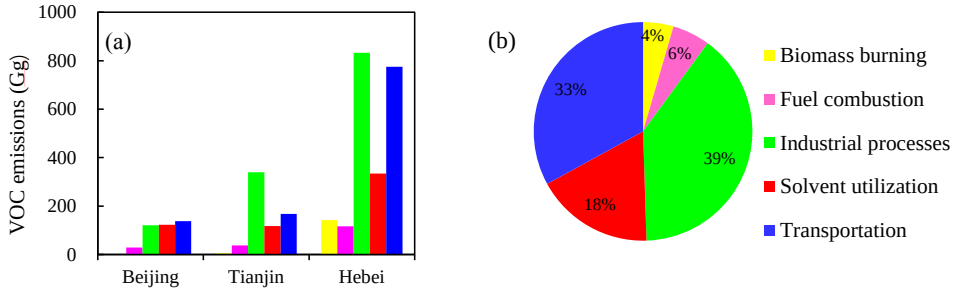

Figure 3. Source contributions to the total VOC emission in the Beijing, Tianjin, Hebei provinces (a) and the BTH region (b), China.

Atmos. Chem. Phys. Discuss., https://doi.org/10.5194/acp-2018-1133
Manuscript under review for journal Atmos. Chem. Phys.
Discussion started: 3 January 2019

625

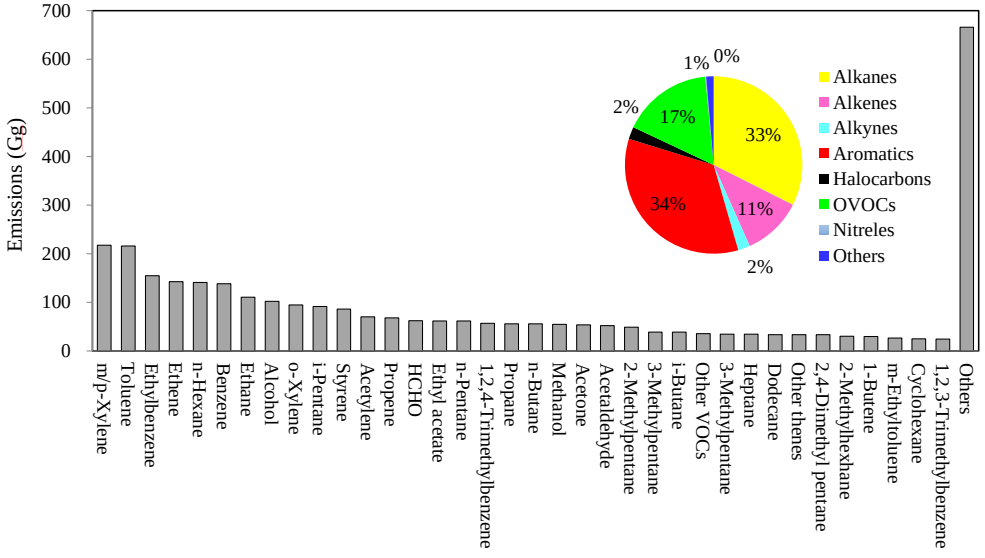

Figure 4. VOC emissions in the BTH region, China.

Atmos. Chem. Phys. Discuss., https://doi.org/10.5194/acp-2018-1133
Manuscript under review for journal Atmos. Chem. Phys.
Discussion started: 3 January 2019

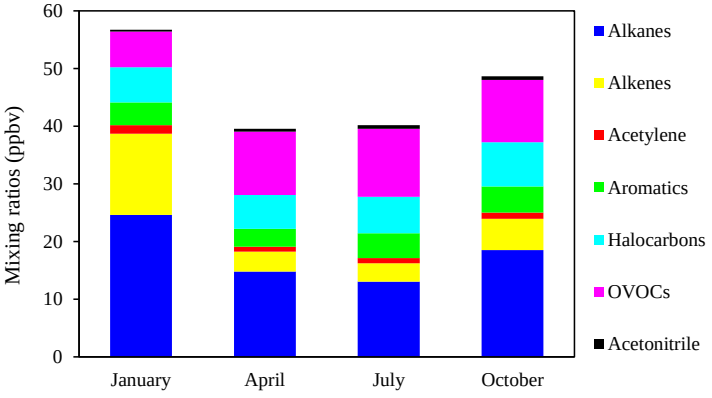

630 **Figure 5. Mixing ratios and compositions of VOCs (ppbv) measured at the PKU site during the four seasons and throughtout the entire study period.**

Atmos. Chem. Phys. Discuss., https://doi.org/10.5194/acp-2018-1133
Manuscript under review for journal Atmos. Chem. Phys.
Discussion started: 3 January 2019

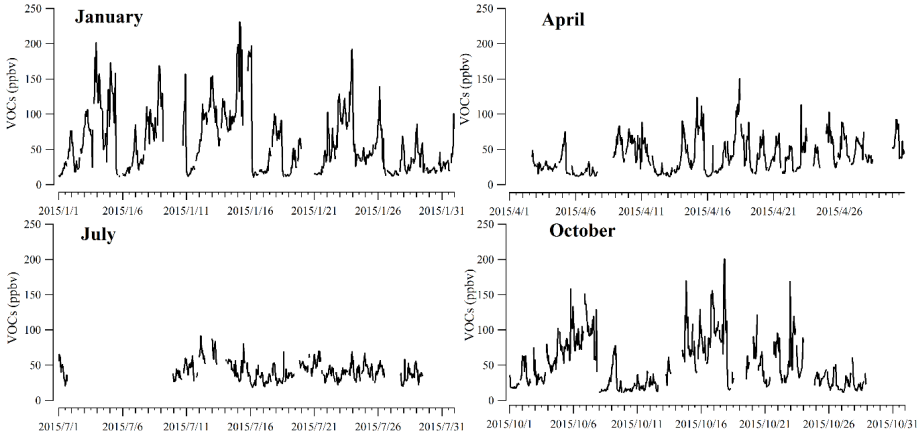

Figure 6. Time series of mixing ratios of VOCs in January, April, July, and October 2015.

Atmos. Chem. Phys. Discuss., https://doi.org/10.5194/acp-2018-1133
Manuscript under review for journal Atmos. Chem. Phys.
Discussion started: 3 January 2019

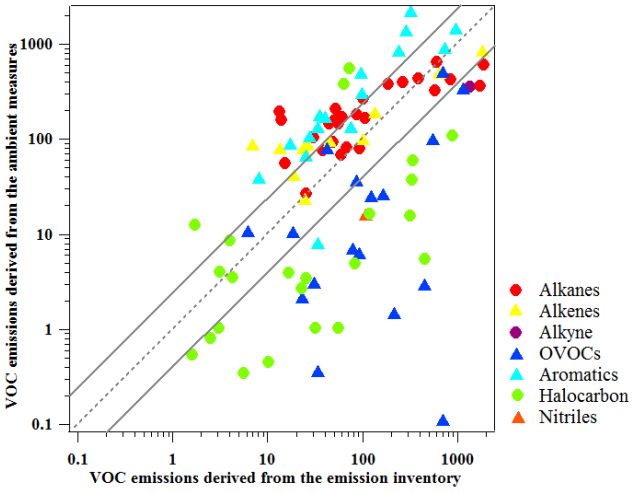

Figure 7. Comparisons of VOC annual emissions (ton) derived from the ambient measures and emission inventory for the PKU site (0.25 ° × 0.25 °grid).

Atmos. Chem. Phys. Discuss., https://doi.org/10.5194/acp-2018-1133
Manuscript under review for journal Atmos. Chem. Phys.
Discussion started: 3 January 2019

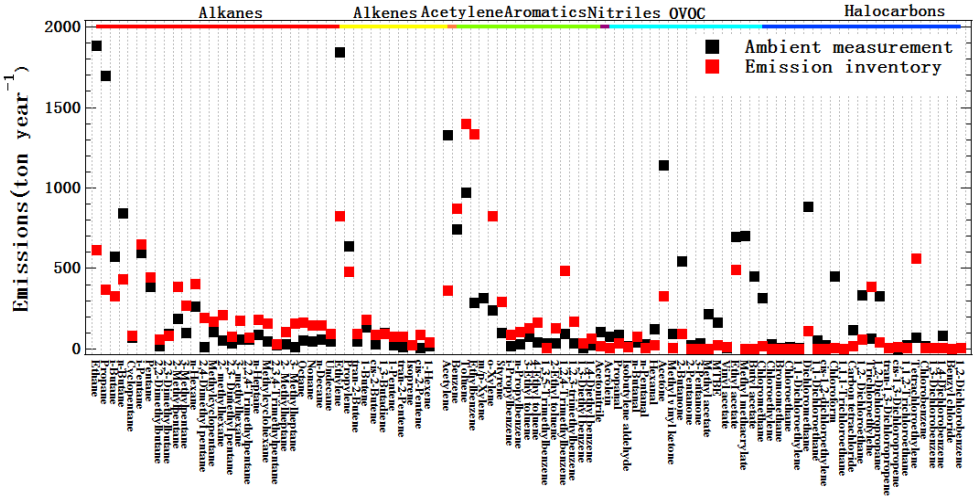

636

637 **Figure 8. Comparisons of individual species emissions (ton) derived from the ambient measures and emission inventory**
638 **for the PKU site (0.25 ° × 0.25 °grid).**

Atmos. Chem. Phys. Discuss., https://doi.org/10.5194/acp-2018-1133
Manuscript under review for journal Atmos. Chem. Phys.
Discussion started: 3 January 2019

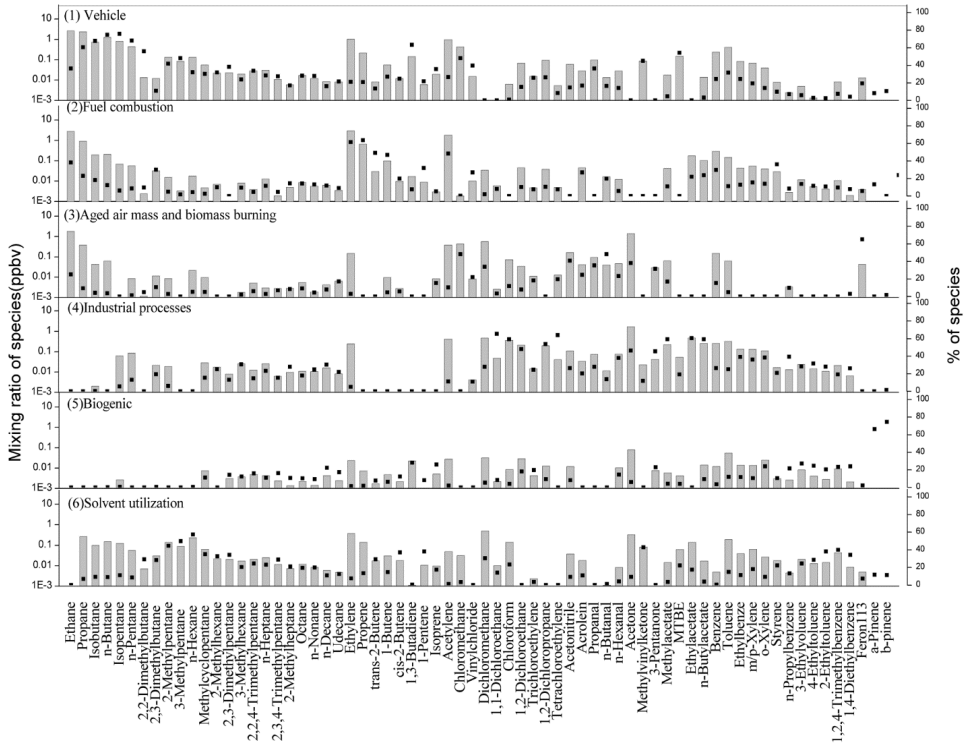

Figure 9.Source profiles for VOCs in the PKU site calculated by PMF (bars: mixing ratio of species; dots: % of species).

Atmos. Chem. Phys. Discuss., https://doi.org/10.5194/acp-2018-1133
Manuscript under review for journal Atmos. Chem. Phys.
Discussion started: 3 January 2019

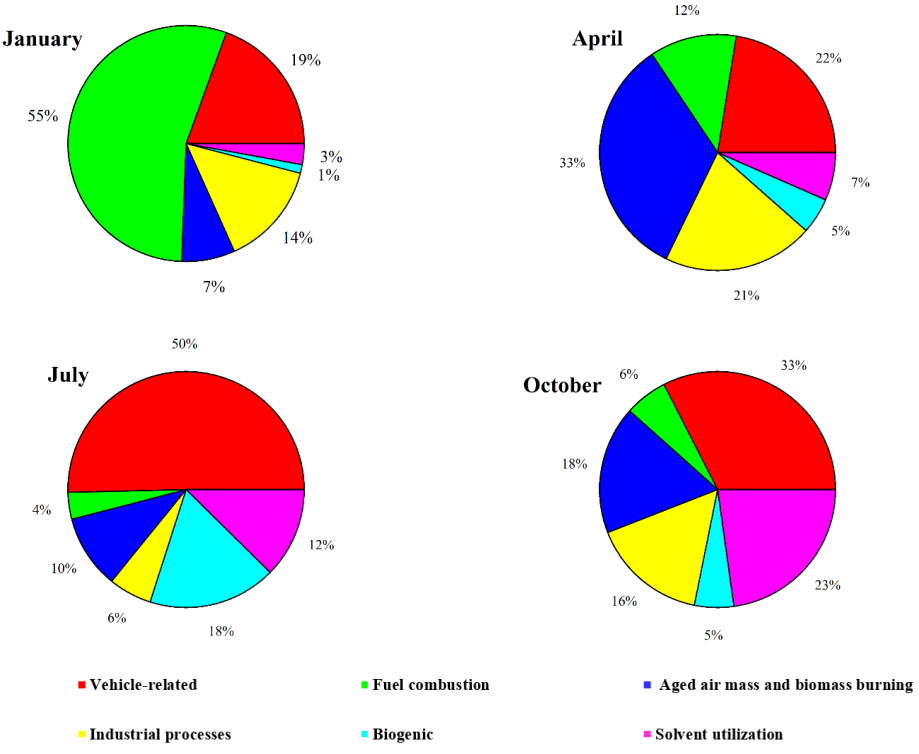

Figure 10. Relative contributions (%) of the six sources identified by PMF analysis in January, April, July, and October of 2015.

Atmos. Chem. Phys. Discuss., https://doi.org/10.5194/acp-2018-1133
Manuscript under review for journal Atmos. Chem. Phys.
Discussion started: 3 January 2019

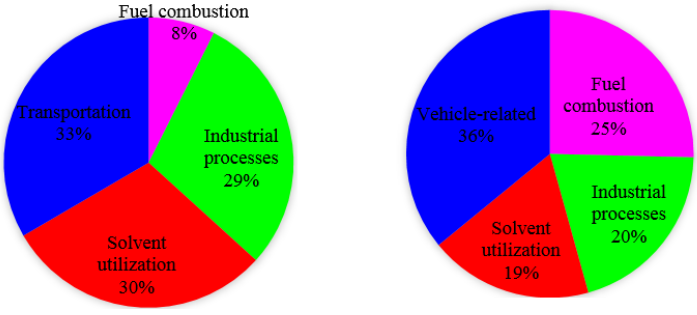

Figure 11. Comparsion of VOC source structure in the emission inventory (left) and the PMF results (right).

Atmos. Chem. Phys. Discuss., https://doi.org/10.5194/acp-2018-1133
Manuscript under review for journal Atmos. Chem. Phys.
Discussion started: 3 January 2019

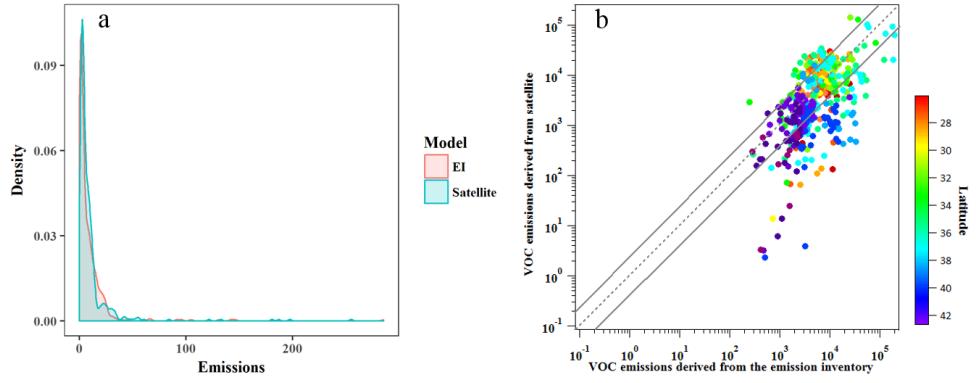

Figure 12. Comparisons between emissions from the EF-derived emission inventory and the satellite-derived emission inventory.

Atmos. Chem. Phys. Discuss., https://doi.org/10.5194/acp-2018-1133
Manuscript under review for journal Atmos. Chem. Phys.
Discussion started: 3 January 2019

650

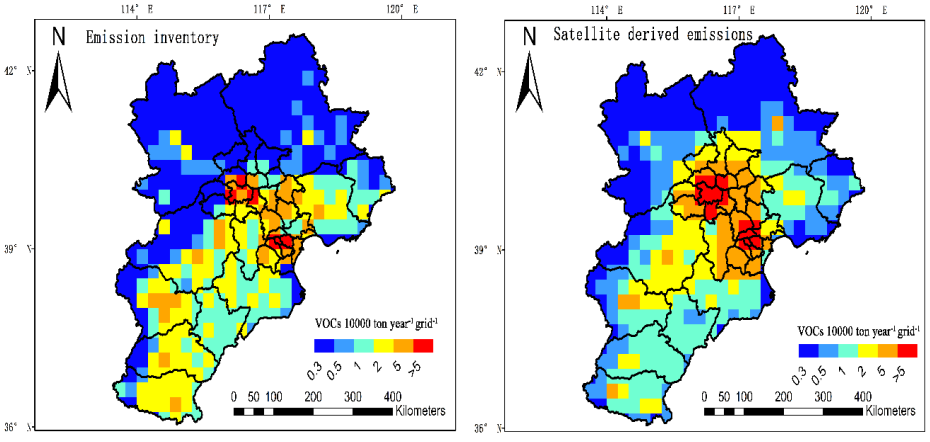

Figure 13. Comparision between spatial distribution of VOC emissions obtained from the EF-derived emission inventory and the satellite-derived emission inventory with a 0.25 ° × 0.25 ° spatial resolution.

Atmos. Chem. Phys. Discuss., https://doi.org/10.5194/acp-2018-1133
Manuscript under review for journal Atmos. Chem. Phys.
Discussion started: 3 January 2019

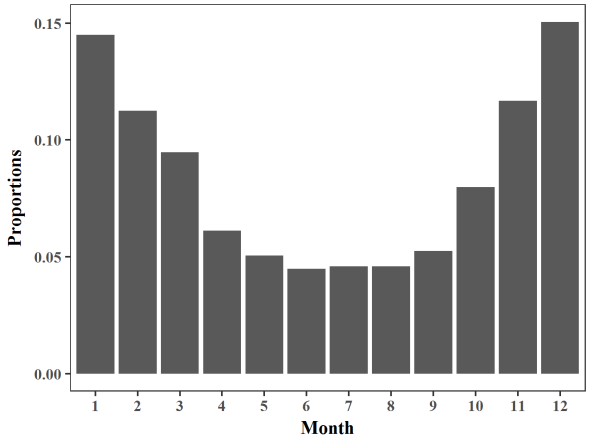

655 **Figure 14. Monthly profiles of VOC emissions from the satellite-derived emission inventory.**